Infrared Faraday rotation of n-type InSb

H. J. Jiménez-González,* R. L. Aggarwal,* and G. Favrot
Francis Bitter National Magnet Laboratory and Department of Physics, Massachusetts Institute of Technology, Cambridge, Massachusetts 02139
(Received 28 April 1993; revised manuscript received 15 October 1993)

The Faraday rotation of n-type InSb has been measured for wavelengths between 8.0 and 13.0 μm at 9 K, using magnetic fields up to 150 kG. Measurements were made on samples with nominal carrier concentration of 1×10^{14}, 6×10^{14}, 1×10^{15}, and 5×10^{15} cm^{-3}. The experimental results have been successfully analyzed in terms of interband and intraband transitions at the Γ point in the Brillouin zone, using a quantum-mechanical treatment. The four-band $\mathbf{k} \cdot \mathbf{p}$ Pidgeon and Brown model was used to calculate the energy levels and the matrix elements for these transitions.

I. INTRODUCTION

The Faraday rotation in InSb was the subject of considerable attention from the late 1950s through the mid 1960s.[1–11] Smith, Moss, and Taylor[3] measured the wavelength dependence of the Faraday rotation in n-type InSb. For carrier concentrations $N_e \gtrsim 1 \times 10^{16}$ cm^{-3} and long wavelengths $\lambda \gtrsim 12$ μm, their measurements exhibited the expected λ^2 behavior predicted by the classical expression, derived in 1955 by Mitchell,[12] for the plasma contribution due to the cyclotron motion of the conduction electrons in a magnetic field.

In the same paper they noted that the interband effect was of opposite sign to that of the free carriers. This result was confirmed by Brown and Lax,[13] and Lax.[14] In 1962, Boswarva, Howard, and Lidiard[6] provided a quantum-mechanical treatment using time-dependent perturbation theory in which they derived an expression for the dielectric tensor of InSb in the presence of a magnetic field. Subsequent papers by Halpern, Lax, and Nishina,[8] Boswarva and Lidiard,[9] and Roth[10] used quantum-mechanical treatments to calculate the Faraday rotation of InSb at low magnetic fields. A free-carrier spin-induced contribution to the Faraday rotation, proportional to the average spin alignment, was first observed in CdS by Romestain, Geschwind, and Devlin[15] in 1975, later in $Hg_{1-x}Cd_xTe$ and $Hg_{1-x}Mn_xTe$ by Yuen *et al.*[16] in 1987, and in InSb by Aggarwal, Lucey, and Ryan-Howard.[17]

The total Faraday rotation in n-type InSb can be regarded as consisting of three contributions as illustrated in Fig. 1. The *plasma* contribution results from virtual intraband transitions where both the initial and intermediate states are in the conduction band. The *interband* contribution arises from virtual transitions between initial states in the valence bands and intermediate states in the conduction band assuming the latter to be empty. The *spin* contribution accounts for the effect of the occupation of conduction-band states ignored in the interband calculation and it results from virtual transitions from occupied states in the conduction band with intermediate states in the valence band.

In this paper, we report a study of the Faraday rotation as a function of wavelength, carrier concentration, and magnetic field. Measurements were made for wavelengths between 8.0 and 13.0 μm at 9 K on n-type samples with nominal carrier concentrations of 1×10^{14}, 6×10^{14}, 1×10^{15}, and 5×10^{15} cm^{-3} using magnetic fields up to 150 kG.

The quantitative analysis has been carried out following the approach of Halpern, Lax, and Nishina.[8] The energy bands and matrix elements needed for the calculation of the Faraday rotation were obtained using the 4-band $\mathbf{k} \cdot \mathbf{p}$ model of Pidgeon and Brown[18] (PB). This calculation gives good results for the spin, plasma, and interband contributions, accounting for population-induced quantum oscillation effects observed at low magnetic fields.

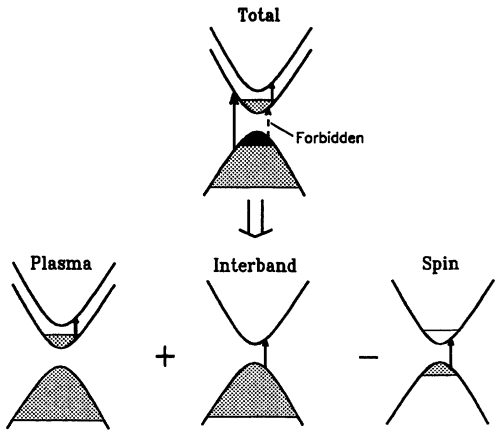

FIG. 1. Diagram illustrating the transitions that give rise to the plasma, interband, and spin contributions.

II. THEORETICAL BACKGROUND

A. Faraday rotation: Quantum-mechanical treatment

We consider linearly polarized light propagating through a material of length L in the direction of the applied magnetic field $\mathbf{B}$. After passing through the material, the electric field vector makes an angle Θ_F with the initial polarization direction.

Faraday rotation results from the difference in phase velocity of left- (LCP) and right- (RCP) circularly polarized light propagating through a medium along $\mathbf{B}$. It follows that the Faraday rotation is given by

$$\Theta_F = \frac{\omega}{2c}(n_- - n_+)L, \tag{1}$$

where ω is the angular frequency of the light, c is the speed of light in vacuum, and n_- and n_+ are the refractive indices for LCP and RCP light, respectively. We are using the convention where right- and left-circular polarizations correspond to positive and negative helicity, respectively.[19]

At frequencies where the absorption is small, the above equation can be written as

$$\Theta_F = \frac{\omega}{4n_0c}(\epsilon_- - \epsilon_+)L, \tag{2}$$

where n_0 is the zero-field refractive index, and ϵ_- and ϵ_+ are the real parts of the dielectric constants for LCP and RCP light, respectively. Using the relation

$$\epsilon = 1 + \frac{4\pi i\sigma}{\omega}, \tag{3}$$

between the complex dielectric constant and the electrical conductivity σ, we can calculate the Faraday rotation by extracting the conductivity from the quantum-mechanical expectation value of the current density operator[20]

$$\mathbf{j} = \frac{1}{2}(\psi^*\mathbf{v}\psi - \psi\mathbf{v}\psi^*), \tag{4}$$

where $\mathbf{v}$ is the velocity operator, and ψ is an eigenstate of the perturbed Hamiltonian. Proceeding in this fashion we obtain

$$\epsilon_- - \epsilon_+ = \frac{4\pi e^2}{m\omega^2}\sum_i (A_{ii}^- - A_{ii}^+)f_i, \tag{5}$$

where m is the free-electron mass, e is the magnitude of the electron charge, the index i denotes the initial states, and A_{ii}^+ and A_{ii}^- are the transition amplitudes for the two circular polarizations of the form

$$A_{ii}^{\pm} = m\sum_{i'}\left[\frac{(\hat{\mathbf{e}}_\pm^*\cdot\mathbf{v})_{ii'}(\hat{\mathbf{e}}_\pm\cdot\mathbf{v})_{i'i}}{\hbar(\omega-\omega_{i'i})} - \frac{(\hat{\mathbf{e}}_\pm\cdot\mathbf{v})_{ii'}(\hat{\mathbf{e}}_\pm^*\cdot\mathbf{v})_{i'i}}{\hbar(\omega+\omega_{i'i})}\right](1-f_{i'}), \tag{6}$$

where the index i' denotes the intermediate states, and f_i and $f_{i'}$ are the occupation probabilities for the initial and intermediate states, respectively. Here the state wave functions have been normalized to unit volume. $\hat{\mathbf{e}}_\pm$ are the unit polarization vectors for the RCP and LCP light, respectively and $\hbar$ is Planck's constant divided by 2π. Using the relationship $(\hat{\mathbf{e}}_\pm^*\cdot\mathbf{v})_{i'i} = (\hat{\mathbf{e}}_\pm\cdot\mathbf{v})_{ii'}^*$ and combining Eqs. (5) and (6) with Eq. (2), we obtain

$$\Theta_F = -\frac{\pi\hbar e^2}{n_0c}\sum_i\sum_{i'}\left[\frac{|(v_+)_{i'i}|^2 - |(v_-)_{i'i}|^2}{\hbar^2(\omega_{i'i}^2-\omega^2)}\right]\times f_i(1-f_{i'})L, \tag{7}$$

where

$$v_\pm \equiv v_x \pm iv_y = \sqrt{2}(\hat{\mathbf{e}}_\pm\cdot\mathbf{v}).$$

The evaluation of the above expression for Θ_F requires the knowledge of the energy levels and matrix elements in InSb as a function of the applied magnetic field, as considered in the following section.

B. Energy levels and matrix elements

In the narrow-gap semiconductor InSb, the conduction band Γ_6, light- and heavy-hole valence bands Γ_8, and spin-orbit split-off valence band Γ_7 are closely spaced at the center of the Brillouin zone.[21] The fundamental energy gap E_g between the Γ_6 and Γ_8 bands is ~ 0.235 eV and the spin-orbit splitting Δ between the Γ_8 and Γ_7 bands is ~ 0.8 eV at liquid helium temperature. Therefore, it is a good approximation to consider only this set of strongly interacting bands exactly and treat interactions with all other bands in an approximate fashion to order k^2. To calculate the energies of the Landau subbands induced by the application of an external magnetic field, we use the PB model,[18] which extends Kane's[22] effective mass theory to the case of a finite magnetic field, and incorporates the treatment of the valence band introduced by Luttinger and Kohn[23] and Luttinger.[24] We used the axial model Hamiltonian[18] D_0, generalized to the case of finite wave vector k_ζ in the direction of $\mathbf{B}$.[25,26]

We measured Faraday rotation with the magnetic field applied along the [111], [211], [110] crystal axes. However, anisotropy effects were too small to resolve from uncertainties in the measurements and we carried out the calculations only for the case of $\mathbf{B} \parallel [111]$. This direction also gives the best match to the pseudopotential energy bands at $B = 0$.[27]

When spin degeneracy at the Γ point is included we get an 8×8 Hamiltonian that can be divided into blocks[28,29]

$$\mathcal{H} = \begin{pmatrix} \mathcal{H}_{cc} & \mathcal{H}_{cv} & \mathcal{H}_{cs} \\ \mathcal{H}_{cv}^\dagger & \mathcal{H}_{vv} & \mathcal{H}_{vs} \\ \mathcal{H}_{cs}^\dagger & \mathcal{H}_{vs}^\dagger & \mathcal{H}_{ss} \end{pmatrix}, \tag{8}$$

where $\mathcal{H}_{cc}$, $\mathcal{H}_{vv}$, and $\mathcal{H}_{ss}$ are the (2×2), (4×4), and (2×2) diagonal blocks associated with the Γ_6 conduction, Γ_8 valence, and Γ_7 split-off valence bands, respectively, and $\mathcal{H}_{cv}$, $\mathcal{H}_{cs}$, and $\mathcal{H}_{vs}$ describe the coupling among the three diagonal blocks.

The PB valence-band parameters are related to the

Luttinger parameters[24] by

$$\begin{aligned}\gamma_1 &= \gamma_1^L - E_p/3E_g,\\ \gamma_2 &= \gamma_2^L - E_p/6E_g,\\ \gamma_3 &= \gamma_3^L - E_p/6E_g,\\ \kappa &= \kappa^L - E_p/6E_g,\end{aligned} \tag{9}$$

where $E_p = 2P^2/m$ is the interaction energy[30] associated with the interband momentum matrix element P. We have chosen the band parameters to be consistent with the best known values (in our judgment) for the band gap,[31] spin-orbit splitting,[32] conduction-band g factor[33] g_c, conduction-band effective mass[34] m_c, and light- and heavy-hole valence-band masses[35] m_l and m_h, respectively, as summarized in Table I. In this table we also give various other band parameters[36] including $\bar{\gamma}$ and N_1, which we have adjusted to give the best fit to the experimental results. The conduction-band effective mass and the g factor are related to the PB parameters by[37]

$$\frac{m}{m_c} \equiv 1 + 2F + \frac{1}{3}E_p\left[\frac{2}{E_g} + \frac{1}{E_g+\Delta}\right], \tag{10}$$

$$g_c \equiv 2\left\{1 + 2N_1 - \frac{1}{3}E_p\left[\frac{1}{E_g} - \frac{1}{E_g+\Delta}\right]\right\}. \tag{11}$$

The light- and heavy-hole valence-band effective masses in the spherical model are given by[10]

$$m_{l(h)}^{-1} = \gamma_1^L \pm 2\bar{\gamma}^L. \tag{12}$$

The velocity operators v_+ and v_- are calculated from the PB Hamiltonian, using the prescription[26,38–40]

$$v_+ = 2\frac{\partial \mathcal{H}}{\partial k_-}$$

$$v_- = 2\frac{\partial \mathcal{H}}{\partial k_+}, \tag{13}$$

where $k_\pm = k_\xi \pm ik_\eta$ in the $\xi\eta\zeta$ coordinate frame.

The transition matrix elements can now be computed using the axial model selection rules (M_0 and M_1 transitions of Trebin, Rossler, and Ranvaud[28])

$$v_\pm : |\ell\rangle \rightarrow |\ell \pm 1\rangle, \tag{14}$$

where ℓ is the quantum number associated with the total angular momentum along the ζ direction [denoted N in Eq. (27) of Ref. 28].

We evaluated Eq. (7) by numerical integration over k_ζ and summation over the quantum number ℓ. The wave function at each point in k_ζ is obtained by diagonalization of an (8 × 8) Hamiltonian.

TABLE I. Band parameters used in the model of Pidgeon and Brown.

Parameter	Value
E_g	0.2352 eV[a]
Δ	0.803 eV[b]
g_c	-51.1[c]
m_c/m	0.0136[d]
m_l/m	0.015[e]
m_h/m	0.38[e]
E_p	23.1 eV[f]
γ_1	3.1[g]
$\bar{\gamma}$[h]	-0.20
μ[i]	0.55[g]
κ	-1.3[g]
F	-0.5[c]
N_1	-0.65

[a]Reference 31.
[b]Reference 32.
[c]Reference 33.
[d]Reference 34.
[e]Reference 35.
[f]Reference 25.
[g]Reference 36.
[h]$\bar{\gamma} = \frac{1}{5}(2\gamma_2 + 3\gamma_3)$.
[i]$\mu = \frac{1}{2}(\gamma_3 - \gamma_2)$.

C. Plasma contribution

The plasma contribution to the Faraday rotation in n-type semiconductors is the result of intraband transitions with both initial and intermediate states within the conduction band. This contribution has a positive sign, is proportional to N_e, and has a λ^2 dependence over the measured wavelength region. As we approach the cyclotron frequency the plasma contribution shows resonant behavior. Near resonance, the light first becomes elliptically polarized and at resonance it becomes left-circularly polarized. Thus Faraday rotation becomes undefined in the region of cyclotron resonance.

For the plasma contribution, the index i in Eq. (8) runs over all occupied states in the conduction band and the sum in i' is over all unoccupied states of the conduction band connected by the velocity operators v_+ and v_-. In the quantum limit, only the ground state ($n = 0$, $m_j = 1/2$) is occupied and is connected to the excited state ($n = 1$, $m_j = 1/2$) via v_+.

To obtain the contribution of occupied conduction-band initial states to the Faraday rotation it is necessary to first calculate the chemical potential for any given temperature and carrier concentration. With this knowledge, we then sum over the initial states including those with energy higher than the chemical potential and apply a Fermi-Dirac distribution to properly account for the population effects. When the intermediate states of a transition are in the conduction band as well, there is considerable overlapping between initial and intermediate states. In this case the Fermi-Dirac distribution has to be applied to both initial and intermediate states. The chemical potential of InSb at 0 and 9 K is shown in Fig. 2 for various carrier concentrations. As shown in the figure, thermal effects are significant at $T = 9$ K, having the effect of broadening the cusps seen in the Fermi energy (chemical potential at $T = 0$ K).

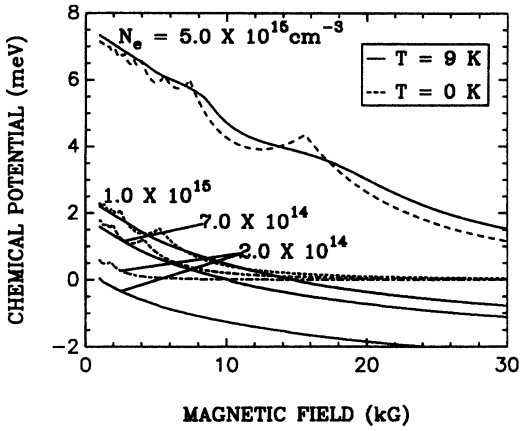

FIG. 2. Chemical potential of InSb at various carrier concentrations for $T = 9$ and 0 K.

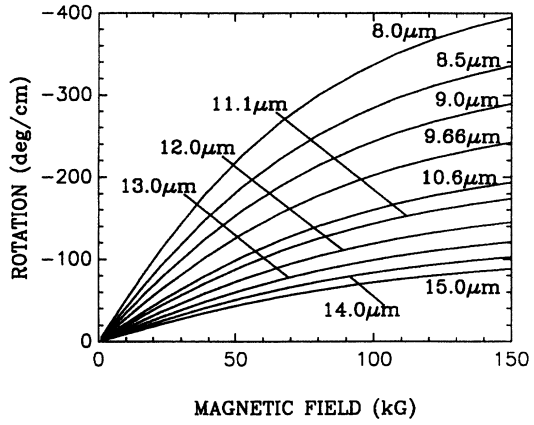

FIG. 3. Calculated interband Faraday rotation as a function of applied magnetic field for various wavelengths in the 8–15-μm range.

D. Interband and spin contributions

The "true" interband Faraday rotation arises from all transitions connecting states in the valence bands to states in the conduction band. However, it is convenient to divide this calculation into a contribution independent of the carrier concentration which in this paper is referred to as the interband contribution and assumes an empty conduction band and a carrier-concentration-dependent contribution due to the occupied conduction-band initial states with intermediate states in the valence bands assuming the latter to be empty. This contribution due to free carrier transitions across the band gap is what has been called the *spin* contribution.[15–17]

1. Interband

In calculating the interband contribution to the Faraday rotation, we will assume a completely empty conduction band and a completely full valence band. We need to sum over all initial states for all values of k_ζ, where ζ is the coordinate along the **B** direction. However, we find that Eq. (7) converges too slowly for practical applications. It is possible, however, to transform Eq. (7) to a form that converges more rapidly,[9]

$$\Theta_F = -\frac{\pi\hbar e^2}{n_0 c}\sum_i\sum_{i'}\frac{\omega^2}{\omega_{i'i}^2}\left[\frac{|(v_+)_{i'i}|^2-|(v_-)_{i'i}|^2}{\hbar^2(\omega_{i'i}^2-\omega^2)}\right]L. \tag{15}$$

This is obtained by substituting the identity

$$\frac{1}{\omega_{i'i}^2-\omega^2}=\frac{1}{\omega_{i'i}^2}+\frac{\omega^2}{\omega_{i'i}^2(\omega_{i'i}^2-\omega^2)},$$

into Eq. (7) and realizing the existence of a sum rule[9] where for every point in k_ζ

$$\sum_i\sum_{i'}\left[\frac{|(v_+)_{i'i}|^2-|(v_-)_{i'i}|^2}{\omega_{i'i}^2}\right]=0. \tag{16}$$

We have verified this result numerically and also shown that the integral of this function with respect to k_ζ converges to zero.

The calculated interband Faraday rotation as a function of the applied magnetic field is shown in Fig. 3 for several wavelengths. It has a negative sign and its magnitude increases monotonically with magnetic field and inversely with wavelength. In Fig. 4 we plot the low-field slope of the Faraday rotation, known as the Verdet constant, as a function of photon energy $\hbar\omega$ which has approximately an ω^2 dependence over the measured frequency range. For comparison, we have included the results of Roth's[10] calculation of the interband Verdet constant. These results are in general qualitative agreement,

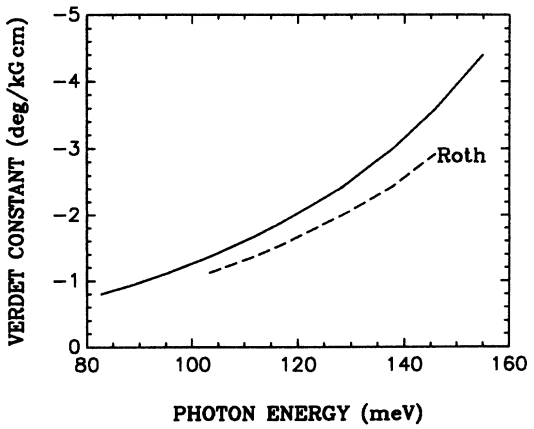

FIG. 4. Calculated low-magnetic-field interband Verdet constant of InSb as a function of photon energy. Also included are the results of Roth's calculation.[10]

although Roth predicts somewhat smaller values for the Verdet constant.

Our model for the Faraday rotation allows the calculation of individual band contributions. For example, we can compare the relative sign and magnitude of the light- and heavy-hole contributions to the interband Faraday rotation. We find that the heavy-hole contribution is ~ 4 times larger than the light-hole contribution and has the opposite sign.

The PB model is limited by the fact that it treats contributions outside of the coupled four-band set only in second-order perturbation theory. This results in unrealistic energy bands for large enough values of k_ζ, or, equivalently, high energies above the lowest conduction subband and below the highest valence subband. By comparing the zero-magnetic-field energy bands of the PB model and those obtained from pseudopotential calculations,[27] we found that the PB model is good up to ~ 1 eV in the conduction band, ~ -1.25 eV in the light-hole band, and ~ -0.5 eV in the heavy-hole band, where the zero of energy is taken at the top of the valence band. By truncating the interband calculation at energies above which the PB model deviates from the pseudopotential calculations we find that the Faraday rotation obtained differs from the result of an untruncated interband calculation by $\sim 4\%$. This indicates that most of the interband contribution comes from the low-energy regions and that the PB model is adequate for the computation of interband Faraday rotation in InSb.

2. *Spin contribution*

The spin contribution to the Faraday rotation has a negative sign, is proportional to N_e, and has an approximate $1/\lambda$-dependence over the measured wavelength region. As noted above, it is the result of interband transitions between occupied initial states in the conduction band and intermediate states in the valence band as allowed by the selection rules [see Eq. (14)]. Conversely, we can think of the spin contribution as the consequence of an incomplete summation over the valence- to conduction-band transitions due to the blocking or occupation of conduction-band states.

The existence of a spin contribution to the Faraday rotation was first pointed out by Romestain, Geschwind, and Devlin[15] in 1975 and was later used by other authors.[16,17] These authors pointed out that the spin contribution is proportional to the average spin $\langle\sigma_z\rangle$, where $\langle\sigma_z\rangle = \frac{1}{2}$ at full magnetization. In Fig. 5 we plot the calculated values of $\langle\sigma_z\rangle$ and the spin contribution to the Faraday rotation divided by N_e. The plots in Fig. 5 show that for low magnetic fields the Faraday rotation is very nearly proportional to $\langle\sigma_z\rangle$.

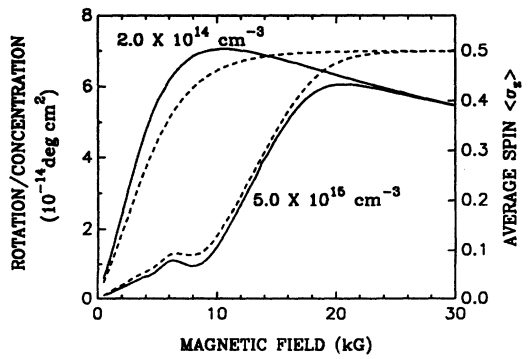

FIG. 5. Calculated average free-electron spin (- - -) and spin contribution to the Faraday rotation divided by N_e (——) at 9.0 K.

III. EXPERIMENTAL PROCEDURE

Faraday rotation measurements at temperature $T = 9$ K were made using a Janis Research[41] helium gas exchange cryostat with a KBr room-temperature window and a ZnSe cold window. A 2-in. bore Bitter solenoid provided dc magnetic fields of up to 150 kG. An air-cooled globar was the radiation source and the linear polarizer used was a PTR Optics[42] wire grid. We used a 0.22-m Spex[43] model 1680B double-grating monochromator. The detector was a liquid-helium-cooled Ge bolometer from Infrared Laboratories.[44] Faraday rotation was measured by recording the power of the transmitted light as a function of magnetic field with a polarizer placed in front of the infrared detector.

Single crystals of n-type InSb, grade 56S, were obtained from Cominco.[45] Four samples with nominal carrier concentrations of 1×10^{14}, 6×10^{14}, 1×10^{15}, and 5×10^{15} cm^{-3} were used for the experiments. The samples were cut and polished, then etched in a 5% solution of bromine in methanol for approximately one minute. The 77-K resistivity ρ, mobility μ, and sample thickness L for these samples are given in Table II.

IV. RESULTS AND DISCUSSION

First we will discuss Faraday rotation at 10.6 μm including the three contributions discussed above. The agreement between the theory and the data is excellent for the four samples at this wavelength. Figure 6 shows the results for $N_e = 5.0 \times 10^{15}$ cm^{-3}. The plasma contri-

TABLE II. Characteristics of InSb samples at 77 K.

N_e (cm^{-3})	ρ (ohm-cm)	μ (cm^2/V·s^2)	L (mm)
1.1 - 1.3 $\times 10^{14}$	5.7 - 7.5 $\times 10^{-2}$	7.5 - 8.4 $\times 10^5$	8.1
5.0 - 6.4 $\times 10^{14}$	2.5 - 2.9 $\times 10^{-2}$	3.9 - 4.2 $\times 10^5$	7.1
0.9 - 1.1 $\times 10^{15}$	1.7 - 2.0 $\times 10^{-2}$	3.3 - 3.4 $\times 10^5$	5.6
4.3 - 5.6 $\times 10^{15}$	6.2 - 7.7 $\times 10^{-3}$	1.8 - 2.0 $\times 10^5$	8.1

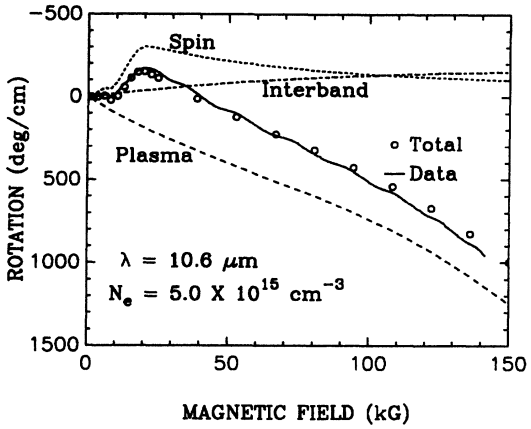

FIG. 6. Faraday rotation of n-type InSb with $N_e = 5.0 \times 10^{15}$ cm^{-3} at 10.6 μm. Interband, plasma, and spin contributions are also shown. The data are shown as a solid line.

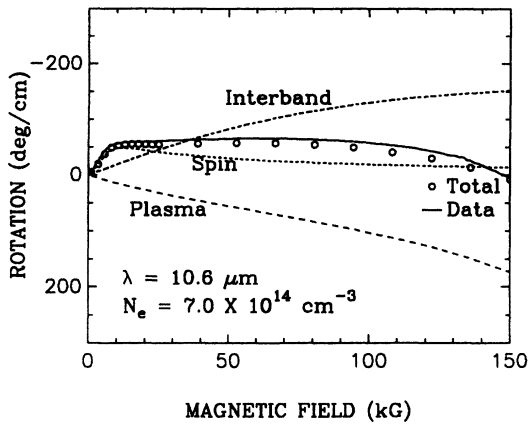

FIG. 8. Faraday rotation of n-type InSb with $N_e = 7.0 \times 10^{14}$ cm^{-3} at 10.6 μm. Interband, plasma, and spin contributions are also shown. The data are shown as a solid line.

bution is linear in B at low magnetic fields and becomes resonant at large values of B. The interband contribution is linear for low values of B and increases sublinearly for high magnetic fields as a consequence of the widening of the band gap which moves the transitions away from resonance. The spin contribution displays the quantum oscillations seen in the chemical potential.[46,47] The maximum at $\sim$ 19 kG corresponds to the Fermi level falling into the lowest Landau subband. The smaller peak at $\sim$ 8 kG corresponds to the Fermi level reaching the $n = 0$, $s = -1/2$ Landau subband. After the quantum limit is reached, the spin contribution slowly decreases as the band gap increases, since this is an interband process resonant at E_g and the magnitude of the transition matrix elements and the effective g factor decrease with increasing E_g. The dependence of the spin Faraday rotation on the g factor can be seen from the low-field approximation used by Aggarwal, Lucey, and Ryan-Howard[17] which shows the spin contribution being proportional to the g factor. The total calculated Faraday rotation shows remarkable agreement with experiment for all values of magnetic field.

In Fig. 7 we show the Faraday rotation for $N_e = 1.0 \times 10^{15}$ cm^{-3}. The interband contribution is independent of carrier concentration and thus remains unchanged; however, the plasma and spin contributions have decreased in magnitude because they are controlled by the population of the conduction band. At this carrier concentration, only the last quantum oscillation is evident and occurs at a lower magnetic field than in the case of $N_e = 5.0 \times 10^{15}$ cm^{-3}. At lower carrier concentrations, Figs. 8 and 9 show a trend in which the spin contribution dominates the low-magnetic-field behavior and the interband contribution is dominant at high magnetic

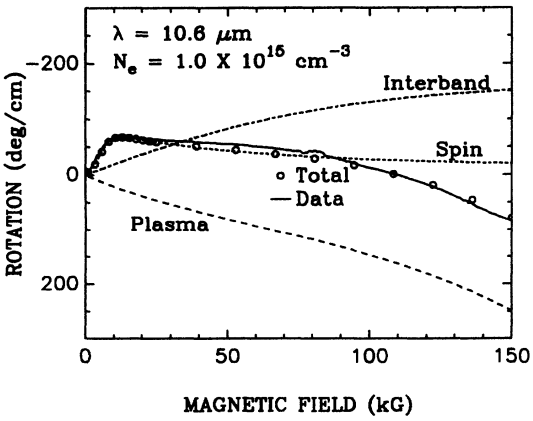

FIG. 7. Faraday rotation of n-type InSb with $N_e = 1.0 \times 10^{15}$ cm^{-3} at 10.6 μm. Interband, plasma, and spin contributions are also shown. The data are shown as a solid line.

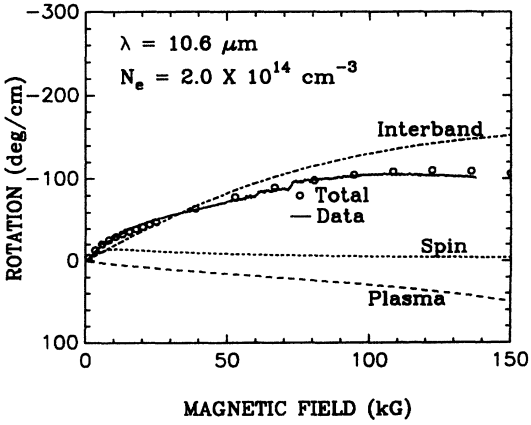

FIG. 9. Faraday rotation of n-type InSb with $N_e = 2.0 \times 10^{14}$ cm^{-3} at 10.6 μm. Interband, plasma, and spin contributions are also shown. The data are shown as a solid line.

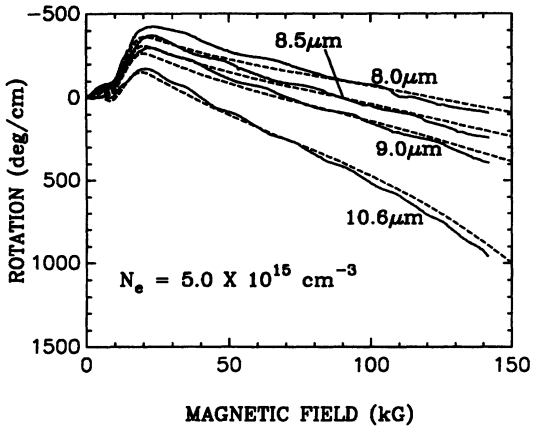

FIG. 10. Faraday rotation of n-type InSb with $N_e = 5.0 \times 10^{15}$ cm^{-3} for various wavelengths. The data are shown as a solid line and the theory is shown as a dashed line.

fields. We have adjusted the carrier concentration used in the calculation to get a better agreement with experiment. To fit the data of the sample with 1.0×10^{14} cm^{-3} nominal concentration we used $N_e = 2.0 \times 10^{14}$ cm^{-3}, and to fit the data of the sample with $N_e = 6.0 \times 10^{14}$ cm^{-3} we used $N_e = 7.0 \times 10^{14}$ cm^{-3}. The adjustment is particularly necessary in order to match the low-magnetic-field spin contribution and the resonant high-magnetic-field plasma contribution to the Faraday rotation. Figure 10 shows the calculated and measured Faraday rotation for various wavelengths for $N_e = 1.0 \times 10^{15}$ cm^{-3}. There is generally good agreement between the calculations and the data for the studied wavelengths. Our data is also in agreement with recently published measurements at 10.6 μm[17].

No attempt was made to find the best set of band parameters for the fitting of the data. A careful selection of parameters may yield a better agreement over the whole range of carrier concentrations.

ACKNOWLEDGMENTS

We express our gratitude to O. W. Shih for his valuable suggestions and discussions. This work is supported in part by the Lincoln Laboratory. The Francis Bitter National Magnet Laboratory is supported by NSF Cooperative Agreement DMR-8813164.

* Also at Lincoln Laboratory, Massachusetts Institute of Technology, Lexington, Massachusetts 02173-9108.
[1] S. D. Smith and T. S. Moss, in *Solid State Physics in Electronics and Telecommunications, Brussels 1958*, edited by M. Désirant and J. L. Michiels (Academic Press, London, 1960), Vol. 2, p. 671.
[2] M. J. Stephen and A. B. Lidiard, J. Phys. Chem. Solids **9**, 43 (1958).
[3] S. D. Smith, T. S. Moss, and K. W. Taylor, J. Phys. Chem. Solids **11**, 131 (1959).
[4] S. D. Smith, C. R. Pidgeon, and V. Prosser, in *Proceedings of the International Conference on the Physics of Semiconductors, Exeter, 1962*, edited by A. C. Stickland (The Physical Society, London, 1962), p. 301.
[5] I. M. Boswarva, Proc. Phys. Soc. London **84**, 389 (1964).
[6] I. M. Boswarva, R. E. Howard, and A. B. Lidiard, Proc. R. Soc. London A **269**, 125 (1962).
[7] J. Kolodziejczak, B. Lax, and Y. Nishina, Phys. Rev. **128**, 2655 (1962).
[8] J. Halpern, B. Lax, and Y. Nishina, Phys. Rev. **134**, A140 (1964).
[9] I. M. Boswarva and A. B. Lidiard, Proc. R. Soc. London A **278**, 588 (1964).
[10] L. M. Roth, Phys. Rev. **133**, A542 (1964).
[11] H. S. Bennet and E. A. Stern, Phys. Rev. **137**, A448 (1965).
[12] E. M. Mitchell, Proc. Phys. Soc. London B **68**, 973 (1955).
[13] R. N. Brown and B. Lax, Bull. Am. Phys. Soc. **4**, 133 (1959).
[14] B. Lax, in *Proceedings of the International Conference on Semiconductor Physics, Prague, 1960* (Academic Press, New York, 1961), p. 321.
[15] R. Romestain, S. Geschwind, and G. E. Devlin, Phys. Rev. Lett. **35**, 803 (1975).
[16] S. Y. Yuen, P. A. Wolff, P. Becla, and D. Nelson, J. Vac. Sci. Technol. **A5**, 3040 (1987).
[17] R. L. Aggarwal, R. F. Lucey, Jr. , and D. P. Ryan-Howard, Appl. Phys. Lett. **53**, 26 (1988).
[18] C. R. Pidgeon and R. N. Brown, Phys. Rev. **146**, 575 (1966).
[19] See J. D. Jackson, *Classical Electrodynamics*, 2nd ed. (Wiley, New York, 1975), p. 274.
[20] G. Baym, *Lectures on Quantum Mechanics* (Benjamin/Cummings, Reading, 1981), p. 503.
[21] G. Dresselhaus, Phys. Rev. **100**, 580 (1955).
[22] E. O. Kane, J. Phys. Chem. Solids **1**, 249 (1957).
[23] J. M. Luttinger and W. Kohn, Phys. Rev. **97**, 869 (1955).
[24] J. M. Luttinger, Phys. Rev. **102**, 1030 (1956).
[25] M. H. Weiler, R. L. Aggarwal, and B. Lax, Phys. Rev. B **17**, 3269 (1978).
[26] R. Grisar, H. Wachernig, G. Bauer, J. Własak, J. Kowalski, and W. Zawadzki, Phys. Rev. B **15**, 4355 (1978).
[27] M. L. Cohen and J. R. Chelikowsky, *Electronic Structure and Optical Properties of Semiconductors* (Springer, Berlin, 1988), p. 120.
[28] H. R. Trebin, U. Rössler, and R. Ranvaud, Phys. Rev. B **19**, 686 (1979).
[29] U. Rössler, Solid State Commun. **49**, 943 (1984).
[30] H. Ehrenreich, J. Appl. Phys. Suppl. **32**, 2155 (1961).
[31] S. Zwerdling, W. H. Kleiner, and J. P. Theriault, J. Appl. Phys. Suppl. **32**, 2118 (1961).
[32] C. R. Pidgeon, S. H. Groves, and J. Feinleib, Solid State Commun. **5**, 677 (1967).
[33] M. W. Goodwin and D. G. Seiler, Phys. Rev. B **27**, 3451 (1982).
[34] R. A. Isaacson, Phys. Rev. **169**, 312 (1969).
[35] J. D. Wiley in *Semiconductors and Semimetals*, edited by

R. K. Willardson and A. C. Beer (Academic Press, New York, 1975), Vol. 10, p. 116.
[36] C. L. Littler and D. G. Seiler, Phys. Rev. B **27**, 7473 (1983).
[37] M. Weiler, J. Magn. Magn. Mater. **11**, 131 (1979).
[38] R. F. Wallis, J. Phys. Chem. Solids **4**, 101 (1958).
[39] E. I. Rashba and V. I. Sheka, Fiz. Tverd. Tela **3**, 1735 (1961) [Sov. Phys. Solid State **3**, 1257 (1961)].
[40] J. J. Stickler, H. J. Zeiger, and G. S. Heller, Phys. Rev. **127**, 1077 (1962).
[41] Janis Research Corp., 2 Jewel Dr., Wilmington, MA 01887.
[42] PTR Optics Corp., 145 Newton St. Waltham, MA 02154.
[43] Spex Industries Inc., Box 798, Metuchen, NJ 08840.
[44] Infrared Laboratories Inc., 1808 East 17th St., Tucson, AZ 85719.
[45] Cominco Electronic Materials, East 15128 Euclid Ave., Spokane, WA 99216.
[46] R. B. Dennis, S. D. Smith, and C. J. Summers, Proc. R. Soc. Lond. A **321**, 303 (1971).
[47] H. A. MacKenzie, R. B. Dennis, D. Voge, and S. D. Smith, Opt. Commun. **34**, 205 (1980).

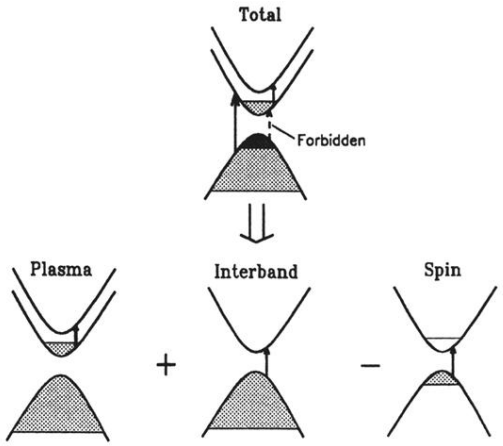

FIG. 1. Diagram illustrating the transitions that give rise to the plasma, interband, and spin contributions.